

CO₂ Activation

How to cite:

International Edition: doi.org/10.1002/anie.202001292

German Edition: doi.org/10.1002/ange.202001292

Carbon Dioxide Activation at Metal Centers: Evolution of Charge Transfer from Mg⁺ to CO₂ in [MgCO₂(H₂O)_n]⁺, n = 0–8

Erik Barwa[†], Tobias F. Pascher[†], Milan Ončák,^{*} Christian van der Linde, and Martin K. Beyer*

Dedicated to Prof. Dr. Dr. Gereon Niedner-Schatteburg on the occasion of his 60th birthday.

Abstract: We investigate activation of carbon dioxide by singly charged hydrated magnesium cations Mg⁺(H₂O)_n through infrared multiple photon dissociation (IRMPD) spectroscopy combined with quantum chemical calculations. The spectra of [MgCO₂(H₂O)_n]⁺ in the 1250–4000 cm⁻¹ region show a sharp transition from n = 2 to n = 3 for the position of the CO₂ antisymmetric stretching mode. This is evidence for the activation of CO₂ via charge transfer from Mg⁺ to CO₂ for n ≥ 3, while smaller clusters feature linear CO₂ coordinated end-on to the metal center. Starting with n = 5, we see a further conformational change, with CO₂⁻ coordination to Mg²⁺ gradually shifting from bidentate to monodentate, consistent with preferential hexa-coordination of Mg²⁺. Our results reveal in detail how hydration promotes CO₂ activation by charge transfer at metal centers.

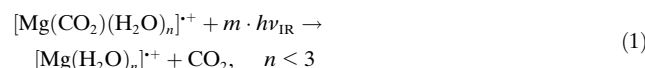
Due to its infrared (IR) active modes,^[1] CO₂ is the major contribution to the anthropogenic greenhouse effect.^[2] Its chemical inertness limits its use as chemical feedstock,^[3] with CO₂⁻ as a key intermediate in many processes.^[4] CO₂⁻ in the gas phase is metastable and decays by autodetachment.^[5] However, solvation efficiently stabilizes this radical anion in small clusters.^[6] Gas phase studies on CO₂ activation have been reviewed recently by Weber^[5a,7] and Schwarz.^[8] These cluster experiments serve as a bridge between the gas and condensed phase.^[9] Uggerud, Asmis and co-workers demonstrated Grignard analogues in the gas phase and identified a bidentate binding motif in the [ClMgCO₂]⁻ complex by infrared spectroscopy.^[10] In this case, liberation of CO was observed after reaction with water.^[10a]

Collision-induced dissociation (CID) experiments and theoretical calculations determined the bond dissociation

energies of Mg⁺ in small water clusters.^[11] Hydrated singly-charged magnesium cations undergo an intracluster reaction within a certain size regime forming MgOH(H₂O)_{n-1}⁺.^[12] Several reactivity and photochemical studies on Mg⁺(H₂O)_n confirmed the coexistence of Mg²⁺ and a hydrated electron for n > 15.^[13] Quantum chemical calculations have corroborated the existence of Mg²⁺/O₂⁻ and Mg²⁺/CO₂⁻ ion pairs in clusters containing 3 and 16 water molecules.^[13h,i] Infrared spectroscopy is an excellent tool for the structural investigation of metal–CO₂ interactions in clusters such as M^{+(CO₂)_n(M = Mg, Al, Si, V, Fe, Co, Ni, Rh, Ir),^[14] or M^{-(CO₂)_n(M = Ti, Mn, Fe, Co, Ni, Cu, Ag, Au, Sn, Bi).^[15] A number of IR spectroscopic studies of hydrated ions M^{+/-}(H₂O)_n have also been performed.^[16] The neutral MgCO₂ complex in helium nanodroplets has been investigated, showing no evidence for charge transfer.^[17] In addition, IR spectroscopy of the hydrated bicarbonate anion HCO₃⁻(H₂O)₁₋₁₀ and the radical anions CO₂⁻(H₂O)₂₋₆₁ and (CO₂)_n⁻ has been performed.^[18] Utilizing matrix isolation, two absorptions of CO₂⁻ have been observed in a neon matrix.^[19]}}

Here, we investigate CO₂ activation in [MgCO₂(H₂O)_n]⁺ clusters, n = 0–8. We probe CO₂ and CO₂⁻ vibrational modes as well as H₂O bending and stretching modes in the 1250–4000 cm⁻¹ region in an FT-ICR mass spectrometer via infrared multiple photon dissociation (IRMPD) spectroscopy. Quantum chemical calculations provide an interpretation of the measured spectra.

IRMPD spectra of [Mg(CO₂)(H₂O)_n]⁺ with the ICR cell cooled to 80 K are shown in Figure 1 for n ≤ 3. For these cluster sizes, fragmentation proceeds by CO₂ loss, reaction (1).



For the smallest clusters [Mg(CO₂)(H₂O)_n]⁺, n = 0–2, the IR spectra indicate the presence of a linear, largely unperturbed CO₂ ligand. The strong absorption at ≈ 2370 cm⁻¹ corresponds to the antisymmetric CO₂ stretch, $\nu_{\text{anti}}(\text{C}-\text{O})$, previously observed in [MgCO₂Ar]⁺.^[14b] Additionally, weak bands separated by ≈ 35–55 cm⁻¹ above and below this band are recorded. For n = 0, 1, the branch with lower energy has smaller intensity. These transitions are interpreted to arise due to CO₂ hindered rotation, $\nu_{\text{hr}}(\text{CO}_2)$, calculated to lie at 58 cm⁻¹ (n = 0) within the harmonic approximation. Thus, the higher-energy branch arises as a combination of $\nu_{\text{anti}}(\text{C}-\text{O})$ and $\nu_{\text{hr}}(\text{CO}_2)$. The lower-energy branch corresponds to the hot-band transition, starting with one vibrational quantum in

[*] M. Sc. E. Barwa,^[†] M. Sc. T. F. Pascher,^[†] Dr. M. Ončák, Dr. C. van der Linde, Prof. Dr. M. K. Beyer
Institut für Ionenphysik und Angewandte Physik, Universität Innsbruck
Technikerstraße 25, 6020 Innsbruck (Austria)
E-mail: milan.oncak@uibk.ac.at
martin.beyer@uibk.ac.at

[†] These authors contributed equally to this work.

Supporting information and the ORCID identification number(s) for the author(s) of this article can be found under:
<https://doi.org/10.1002/anie.202001292>.

© 2020 The Authors. Published by Wiley-VCH Verlag GmbH & Co. KGaA. This is an open access article under the terms of the Creative Commons Attribution License, which permits use, distribution and reproduction in any medium, provided the original work is properly cited.

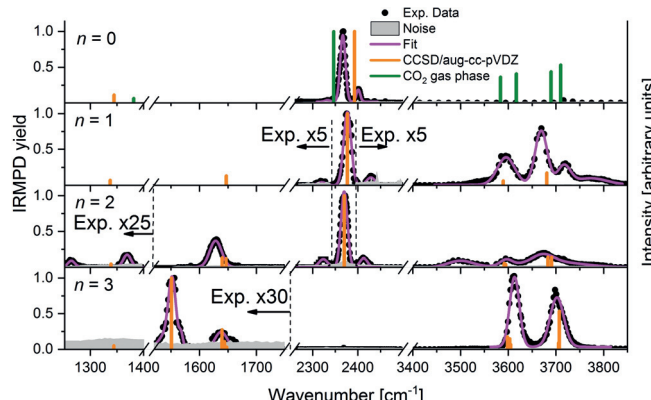


Figure 1. Measured IRMPD spectra of $[\text{MgCO}_2(\text{H}_2\text{O})_n]^+$, $n = 0-3$, at $T \approx 80$ K. Fragmentation proceeds according to reaction (1). IR transitions calculated at the CCSD/aug-cc-pVDZ level for **a** ($n = 0-2$) and **b** ($n = 3$) isomers, respectively, see Figure 2 for structures, are shown as orange bars; scaling of 0.988 was used below 2500 cm^{-1} whereas a factor of 0.95 is used above due to strong anharmonicity of O-H stretching, see Supporting Information for details. Absorption maxima of a measured CO_2 spectrum^[20] are added as green bars for comparison.

$\nu_{\text{hr}}(\text{CO}_2)$. This coupling resembles the situation in $\text{HCO}_2^-(\text{H}_2\text{O})$.^[21] Further absorptions are observed in the $3450-3800\text{ cm}^{-1}$ region for $n \geq 1$. Symmetric and antisymmetric O-H stretch vibrations dominate this region, slightly blue-shifted compared to O-H stretch vibrations in $\text{Mg}^{+}(\text{H}_2\text{O})\text{Ar}$,^[22] with contributions from the well-known Fermi resonances of CO_2 .^[20]

Calculated structures of low-lying isomers are shown in Figure 2. Several isomer classes were considered: Isomer **a** with a linear CO_2 for $n \leq 4$; isomers **b** and **c** with an activated CO_2 possessing a bidentate motif $\eta^2\text{-O}$ and a monodentate motif $\eta^1\text{-O}$, respectively; isomer **d** featuring a solvent-separated $\text{Mg}^{2+}/\text{CO}_2^-$ ion pair for $n \geq 5$.^[13h] As long as the unpaired electron stays on magnesium, asymmetric solvation is preferred, similar to $\text{Mg}^{+}(\text{H}_2\text{O})_n$.^[12b] IR transitions calculated at the CCSD/aug-cc-pVDZ level in harmonic approximation for structures **0a**, **Ia** and **IIa** reproduce the main features of the measured spectra, Figure 1. The position of CO_2 vibrations after complexation to the $\text{Mg}^{+}(\text{H}_2\text{O})_n$ cation,

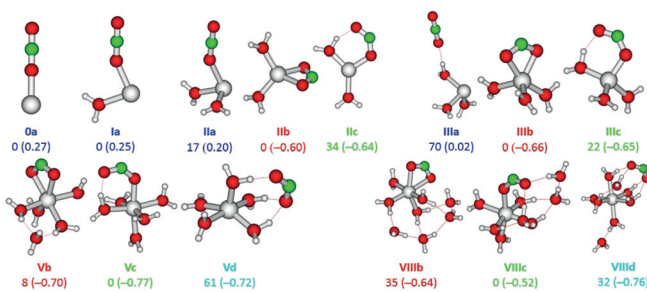


Figure 2. Calculated isomers of $[\text{MgCO}_2(\text{H}_2\text{O})_n]^+$ for $n = 0-3, 5$ and 8 at the M06L/aug-cc-pVDZ level of theory. Relative energies are given in kJ mol^{-1} . The charge on the CO_2 unit (in e) is given in brackets. See Figure S3 for structures with $n = 4, 6, 7$.

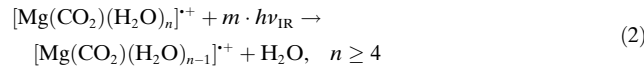
$n = 0-2$, differs only negligibly; thus, CO_2 stays almost uninfluenced by the $\text{Mg}^{+}(\text{H}_2\text{O})_n$ cation. In fact, the IR spectrum of $[\text{Mg}(\text{CO}_2)(\text{H}_2\text{O})_2]^+$ resembles closely a linear combination of CO_2 and $\text{Mg}^{+}(\text{H}_2\text{O})_2$ IR spectra (see Figure S4 in the Supporting Information). Accordingly, calculations also predict no electron transfer to CO_2 for those isomers, with the overall positive charge shared by the carbon dioxide molecule (Figure 2).

While for $n = 0, 1$, the laser system is not powerful enough for IRMPD below 1800 cm^{-1} , we succeeded to measure the IR spectrum also in the $1250-1800\text{ cm}^{-1}$ region for $n = 2$. In the symmetric C-O stretch region, we see bands at 1265 and 1369 cm^{-1} . The calculations predict a splitting of the degenerate CO_2 bending mode due to the interaction with Mg^{+} and water in isomer **IIa** at 654 cm^{-1} and 658 cm^{-1} , along with the fundamental symmetric C-O stretch at 1339 cm^{-1} . The discrepancy arises due to a Fermi resonance between the overtone/combination band of the CO_2 bending with the symmetric C-O stretch vibration within the linear CO_2 molecule. This Fermi interaction is well documented in the literature for CO_2 , shifting the corresponding two vibrations to about 1285 and 1390 cm^{-1} , respectively.^[23] Complexation with Mg^{+} shifts these bands slightly to the red. The remaining band at 1628 cm^{-1} is assigned as water bending mode, in good agreement with calculations (Figure 1).

For $n = 2$, the isomer with activated CO_2 , **IIb**, is already more stable by 17 kJ mol^{-1} compared to **IIa**. However, the activation of CO_2 via electron transfer from a doubly hydrated Mg^{+} center, starting from isomer **IIa**, faces a substantial barrier of 41 kJ mol^{-1} , Figure S5, compared to a CO_2 dissociation energy of 38 kJ mol^{-1} . Thus, isomers **IIb** and **IIc** are not formed in the experiment, as the entropically favored dissociation prevails over CO_2 activation, and only isomer **IIa** is observed. Isomers with activated CO_2 , **IIb/IIc**, also cannot arise from evaporation of a water molecule from the next heavier cluster, $[\text{Mg}(\text{CO}_2)(\text{H}_2\text{O})_3]^+$, as CO_2 loss is preferred for $n \leq 3$, see Table S1, in agreement with experiment.

In the IR spectrum of $n = 3$, we observe a fundamental change: the antisymmetric stretch of CO_2 at $\approx 2370\text{ cm}^{-1}$ shifts to 1552 cm^{-1} . This is clear evidence of CO_2 activation via electron transfer from Mg^{+} to CO_2 , forming an $\text{Mg}^{2+}\cdots\text{CO}_2^-$ ion pair. This electron transfer is driven by the higher water binding energy of Mg^{2+} compared to Mg^{+} .^[11b] The bidentate binding motif **IIb** is energetically slightly preferred over the monodentate **IIc**, while isomer **IIa** containing linear CO_2 is 70 kJ mol^{-1} less stable than **IIb**.

To further probe the influence of the hydration shell on the $\text{Mg}^{2+}/\text{CO}_2^-$ ion pair, we recorded IRMPD spectra of $[\text{Mg}(\text{CO}_2)(\text{H}_2\text{O})_n]^+$ up to $n = 8$ in the $1250-1800\text{ cm}^{-1}$ region at 80 K , shown in Figures 3 and S1. Figure S2 provides spectra at room temperature for comparison. In agreement with the calculated thermochemistry, H_2O evaporates exclusively for $n \geq 4$, reaction (2).



For $n = 3, 4$, we observe a band at 1552 cm^{-1} that can be assigned as the antisymmetric stretch of CO_2^- , $\nu_{\text{anti}}(\text{C}-\text{O})$, in

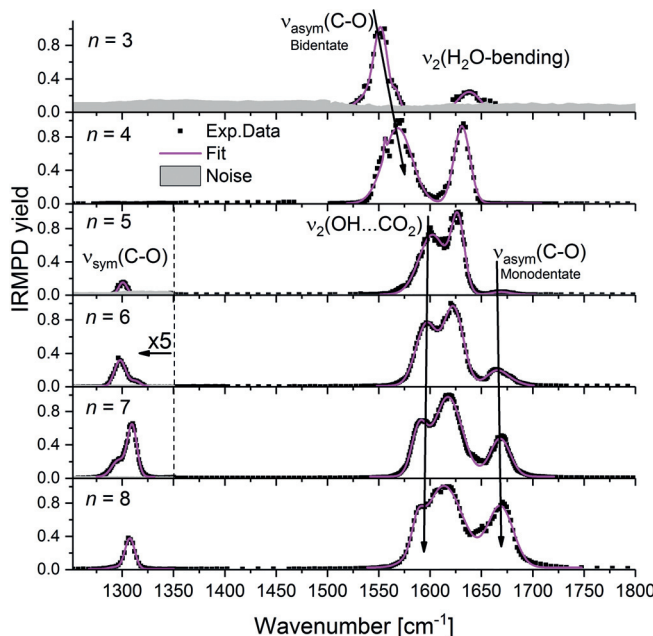


Figure 3. Measured IRMPD spectra of $[\text{Mg}(\text{CO}_2)(\text{H}_2\text{O})_n]^+$ for $n = 3–8$ at $T \approx 80$ K. See the text and reactions (1) and (2) for fragmentation channels.

isomer **IIIb** with bidentate bonding motif.^[18b] The whole absorption band at $1600\text{--}1650\text{ cm}^{-1}$ arises due to water vibrations. Unfortunately, the laser power is not sufficient to observe fragmentation in the $\nu_{\text{sym}}(\text{C}-\text{O})$ symmetric stretching region of the CO_2^- anion in the cooled cell, for $n = 3$ not even at room temperature (Figure S2). This transition is calculated at the M06L/aug-cc-pVDZ levels of theory to be at 1317 and 1259 cm^{-1} for isomers **IIIb** and **IIIc**, respectively. However, isomer **IIIc** should exhibit a very intense absorption at 2863 cm^{-1} , which corresponds to the OH stretch directed to CO_2^- . Due to the lack of this band in the experiment, we conclude to have only isomer **IIIb**, that is, CO_2^- is attached to Mg^{2+} in bidentate manner. Analogously, the structure observed for $n = 4$ is **IVb**; however, the monodentate structure **IVc** is also observed for $n = 4$ at room temperature when more energy is available (Figure S2), evidenced by the additional band at 1678 cm^{-1} . Charge analysis shows that charge transfer takes place from Mg^{2+} , with partial charges on the CO_2 moiety from -0.6 e to -0.7 e .

For $n > 4$, interpretation of the band structure in the $1550\text{--}1750\text{ cm}^{-1}$ region is getting more complicated, since the bidentate, monodentate and solvent separated isomers get closer in energy. In addition, the vibrational frequencies predicted by our quantum chemical calculations strongly depend on the functional, while the relative energies of the isomers are quite robust (see the Supporting Information). We therefore rely on the interpretation of the experimental spectrum based on thermochemical arguments and qualitative trends.

The feature at about 1670 cm^{-1} , indicative of the monodentate structure, emerges for $n = 5$ and becomes more prominent with increasing cluster size. At the same time, the band at $\approx 1560\text{ cm}^{-1}$ is severely weakened, and a new

band at 1600 cm^{-1} appears, which we assign to the H_2O bending mode, $\nu_2(\text{O}-\text{H}\cdots\text{CO}_2)$, involving an interaction of OH groups with the monodentate CO_2^- ligand. The gradual switching between bidentate and monodentate structures from $n = 4$ to $n = 5$ can be rationalized by the preferred hexacoordination of Mg^{2+} , in line with calculated thermochemistry shown in Figures 2 and S3.

A new band appears at about 1300 cm^{-1} for $n > 4$, which we assign to $\nu_{\text{sym}}(\text{C}-\text{O})$ of the monodentate isomers. The structure of the band indicates the presence of several isomers. Interestingly, the change from bidentate to monodentate binding motif does not affect the partial charge of the CO_2^- ligand. With increasing number of water molecules, the water bending region gets more and more congested, reflecting the number of distinguishable H_2O molecules in the cluster and the increasing number of energetically accessible isomers. It is plausible that also solvent-separated isomers contribute to the spectrum, however without a clear spectral assignment. Earlier calculations indicated that solvent-separated ion pair and monodentate contact ion pair structures lie within 10 kJ mol^{-1} for $n = 16$, with the solvent-separated structure slightly preferred.^[13b]

The measured IR spectra of $[\text{Mg}(\text{CO}_2)(\text{H}_2\text{O})_n]^+$ clusters show a clear dependence of CO_2 activation on the number of water molecules. For $n = 2$, although CO_2 activation is thermochemically preferred, it is hindered by a barrier. For $n > 2$, we observe charge transfer from Mg^{2+} to CO_2 , with the resulting CO_2^- coordinated to Mg^{2+} initially in bidentate fashion. With increasing cluster size, monodentate coordination and solvent-separated ion pair structures take over. Our results emphasize the role of water in the activation of CO_2 on metal centers.

Experimental Section

The experiments are performed on a modified 4.7 T FT-ICR Bruker/Spektrospin CMS47X mass spectrometer equipped with an external laser vaporization source.^[24] A pulsed frequency doubled Nd:YAG laser is focused onto a rotating isotopically enriched magnesium target (^{24}Mg , 99.9%). The resulting plasma is entrained into a gas pulse of He, H_2O and CO_2 , undergoing supersonic jet expansion. The temperature of the cylindrical cell is lowered for most experiments to $T \approx 80$ K via liquid nitrogen cooling^[25] to reduce the contribution of black body infrared radiative dissociation (BIRD).^[26] Radiation from tunable OPO laser systems (EKSPLA NT273-XIR, EKSPLO NT277) is coupled into the ICR cell. For evaluation we use the IRMPD yield.^[27] We defined this previously^[28] as $\Sigma(\text{photofragments})/\Sigma(\text{precursor} + \text{photofragments})/P/t$, where P the laser power measured directly after the experiment and t the irradiation time, with each spectrum normalized to the maximum value. Further details on the experimental setup are found in the Supporting Information.

The structure and properties of $[\text{Mg}(\text{CO}_2)(\text{H}_2\text{O})_n]^+$ clusters ($n = 0\text{--}8$) were studied employing CCSD/aug-cc-pVDZ and M06L/aug-cc-pVDZ theory levels, see Supporting Information for benchmarking calculations (Tables S2–S5). While thermochemical values at the CCSD level are reproduced well by selected DFT functionals, vibrational frequencies have a relatively large error, with M06L providing the lowest one on average. Therefore, M06L is used for frequency calculations of larger clusters. Vibrational spectra are scaled by a factor of 0.988 and 0.97 for CCSD and M06L calculations, respectively. A factor of 0.95 is used for CCSD calculations above 2500 cm^{-1} due to the high anharmonicity of O-H stretching vibrations

in hydrated metal cations.^[16k] Wavefunction stabilization was performed, all considered structures represent local minima. Partial charges were calculated within the CHELPG Scheme.^[29] The Gaussian 16 software was employed.^[30]

Acknowledgements

Financial support from the Austrian Science Fund (FWF), project number P28896, is gratefully acknowledged. The computational results have been achieved using the HPC infrastructure LEO of the University of Innsbruck. The tunable OPO systems are part of the Innsbruck Laser Core Facility, financed by the Austrian Federal Ministry of Education, Science and Research.

Conflict of interest

The authors declare no conflict of interest.

Keywords: ab initio calculations · CO₂ activation · hydration · IR spectroscopy · mass spectrometry

How to cite: *Angew. Chem. Int. Ed.* **2020**, *59*, 7467–7471
Angew. Chem. **2020**, *132*, 7537–7541

- [1] A. Sinha, J. E. Harries, *Geophys. Res. Lett.* **1995**, *22*, 2147–2150.
- [2] J. S. Sawyer, *Nature* **1972**, *239*, 23–26.
- [3] R. van Eldik, M. Aresta, *CO₂ Chemistry*, Elsevier, Amsterdam, **2013**.
- [4] a) M. Aresta, A. Dibenedetto, *Dalton Trans.* **2007**, 2975–2992; b) A. S. McNeill, D. A. Dixon, *J. Phys. Chem. A* **2019**, *123*, 1243–1259.
- [5] a) L. G. Dodson, M. C. Thompson, J. M. Weber, *Annu. Rev. Phys. Chem.* **2018**, *69*, 231–252; b) M. Knapp, O. Echt, D. Kreisle, T. D. Märk, E. Recknagel, *Chem. Phys. Lett.* **1986**, *126*, 225–231; c) C. D. Cooper, R. N. Compton, *Chem. Phys. Lett.* **1972**, *14*, 29–32; d) D. Schröder, C. A. Schalley, J. N. Harvey, H. Schwarz, *Int. J. Mass Spectrom.* **1999**, *185*–187, 25–35.
- [6] a) C. E. Klots, R. N. Compton, *J. Chem. Phys.* **1977**, *67*, 1779–1780; b) C. E. Klots, R. N. Compton, *J. Chem. Phys.* **1978**, *69*, 1644–1647; c) C. E. Klots, *J. Chem. Phys.* **1979**, *71*, 4172.
- [7] J. M. Weber, *Int. Rev. Phys. Chem.* **2014**, *33*, 489–519.
- [8] H. Schwarz, *Coord. Chem. Rev.* **2017**, *334*, 112–123.
- [9] X. Yang, A. W. Castleman, *J. Am. Chem. Soc.* **1991**, *113*, 6766–6771.
- [10] a) H. Dossmann (Soldi-Lose), C. Afonso, D. Lesage, J.-C. Tabet, E. Uggerud, *Angew. Chem. Int. Ed.* **2012**, *51*, 6938–6941; *Angew. Chem.* **2012**, *124*, 7044–7047; b) G. B. S. Miller, T. K. Esser, H. Knorke, S. Gewinner, W. Schöllkopf, N. Heine, K. R. Asmis, E. Uggerud, *Angew. Chem. Int. Ed.* **2014**, *53*, 14407–14410; *Angew. Chem.* **2014**, *126*, 14635–14638.
- [11] a) N. F. Dalleska, B. L. Tjelta, P. B. Armentrout, *J. Phys. Chem.* **1994**, *98*, 4191–4195; b) C. W. Bauschlicher, M. Sodipe, H. Partridge, *J. Chem. Phys.* **1992**, *96*, 4453–4463; c) M. Sodipe, C. W. Bauschlicher Jr., *Chem. Phys. Lett.* **1992**, *195*, 494–499.
- [12] a) M. Sanekata, F. Misaizu, K. Fuke, S. Iwata, K. Hashimoto, *J. Am. Chem. Soc.* **1995**, *117*, 747–754; b) H. Watanabe, S. Iwata, K. Hashimoto, F. Misaizu, K. Fuke, *J. Am. Chem. Soc.* **1995**, *117*, 755–763; c) F. Misaizu, M. Sanekata, K. Fuke, S. Iwata, *J. Chem. Phys.* **1994**, *100*, 1161–1170; d) C.-K. Siu, Z. F. Liu, *Chem. Eur. J.* **2002**, *8*, 3177–3186.
- [13] a) C. Berg, M. Beyer, U. Achatz, S. Joos, G. Niedner-Schatteburg, V. E. Bondybey, *Chem. Phys.* **1998**, *239*, 379–392; b) C. Berg, U. Achatz, M. Beyer, S. Joos, G. Albert, T. Schindler, G. Niedner-Schatteburg, V. E. Bondybey, *Int. J. Mass Spectrom. Ion Process.* **1997**, *167*–168, 723–734; c) T.-W. Lam, C. van der Linde, A. Akhgarnusch, Q. Hao, M. K. Beyer, C.-K. Siu, *ChemPlusChem* **2013**, *78*, 1040–1048; d) C. L. Whalley, J. C. G. Martín, T. G. Wright, J. M. C. Plane, *Phys. Chem. Chem. Phys.* **2011**, *13*, 6352–6364; e) M. Ončák, T. Taxer, E. Barwa, C. van der Linde, M. K. Beyer, *J. Chem. Phys.* **2018**, *149*, 044309; f) T. Taxer, M. Ončák, E. Barwa, C. van der Linde, M. K. Beyer, *Faraday Discuss.* **2019**, *217*, 584–600; g) E. Barwa, M. Ončák, T. F. Pascher, T. Taxer, C. van der Linde, M. K. Beyer, *J. Phys. Chem. A* **2019**, *123*, 73–81; h) C. van der Linde, A. Akhgarnusch, C.-K. Siu, M. K. Beyer, *J. Phys. Chem. A* **2011**, *115*, 10174–10180; i) T.-W. Lam, H. Zhang, C.-K. Siu, *J. Phys. Chem. A* **2015**, *119*, 2780–2792.
- [14] a) J. B. Jaeger, T. D. Jaeger, N. R. Brinkmann, H. F. Schaefer, M. A. Duncan, *Can. J. Chem.* **2004**, *82*, 934–946; b) G. Gregoire, N. R. Brinkmann, D. van Heijnsbergen, H. F. Schaefer, M. A. Duncan, *J. Phys. Chem. A* **2003**, *107*, 218–227; c) R. S. Walters, N. R. Brinkmann, H. F. Schaefer, M. A. Duncan, *J. Phys. Chem. A* **2003**, *107*, 7396–7405; d) N. R. Walker, G. A. Grieves, R. S. Walters, M. A. Duncan, *Chem. Phys. Lett.* **2003**, *380*, 230–236; e) N. R. Walker, R. S. Walters, E. D. Pillai, M. A. Duncan, *J. Chem. Phys.* **2003**, *119*, 10471; f) N. R. Walker, R. S. Walters, G. A. Grieves, M. A. Duncan, *J. Chem. Phys.* **2004**, *121*, 10498; g) N. R. Walker, R. S. Walters, M. A. Duncan, *J. Chem. Phys.* **2004**, *120*, 10037; h) G. Gregoire, J. Velasquez, M. A. Duncan, *Chem. Phys. Lett.* **2001**, *349*, 451–457; i) G. Gregoire, M. A. Duncan, *J. Chem. Phys.* **2002**, *117*, 2120; j) A. Iskra, A. S. Gentleman, A. Kartouzian, M. J. Kent, A. P. Sharp, S. R. Mackenzie, *J. Phys. Chem. A* **2017**, *121*, 133–140; k) M. A. Duncan, *Int. Rev. Phys. Chem.* **2003**, *22*, 407–435; l) A. M. Ricks, A. D. Brathwaite, M. A. Duncan, *J. Phys. Chem. A* **2013**, *117*, 11490–11498.
- [15] a) B. J. Knurr, J. M. Weber, *J. Phys. Chem. A* **2014**, *118*, 10246–10251; b) B. J. Knurr, J. M. Weber, *J. Phys. Chem. A* **2014**, *118*, 8753–8757; c) B. J. Knurr, J. M. Weber, *J. Phys. Chem. A* **2014**, *118*, 4056–4062; d) B. J. Knurr, J. M. Weber, *J. Phys. Chem. A* **2015**, *119*, 843–850; e) M. C. Thompson, J. M. Weber, *J. Phys. Chem. A* **2018**, *122*, 3772–3779; f) M. C. Thompson, J. Ramsay, J. M. Weber, *Angew. Chem. Int. Ed.* **2016**, *55*, 15171–15174; *Angew. Chem.* **2016**, *128*, 15396–15399; g) M. C. Thompson, J. Ramsay, J. M. Weber, *J. Phys. Chem. A* **2017**, *121*, 7534–7542; h) M. C. Thompson, L. G. Dodson, J. M. Weber, *J. Phys. Chem. A* **2017**, *121*, 4132–4138; i) B. J. Knurr, J. M. Weber, *J. Phys. Chem. A* **2013**, *117*, 10764–10771; j) B. J. Knurr, J. M. Weber, *J. Am. Chem. Soc.* **2012**, *134*, 18804–18808; k) L. G. Dodson, M. C. Thompson, J. M. Weber, *J. Phys. Chem. A* **2018**, *122*, 2983–2991.
- [16] a) K. Furukawa, K. Ohashi, N. Koga, T. Imamura, K. Judai, N. Nishi, H. Sekiya, *Chem. Phys. Lett.* **2011**, *508*, 202–206; b) Y. Inokuchi, K. Ohshima, F. Misaizu, N. Nishi, *J. Phys. Chem. A* **2004**, *108*, 5034–5040; c) Y. Inokuchi, K. Ohshima, F. Misaizu, N. Nishi, *Chem. Phys. Lett.* **2004**, *390*, 140–144; d) J. S. Prell, J. T. O'Brien, E. R. Williams, *J. Am. Chem. Soc.* **2011**, *133*, 4810–4818; e) J. T. O'Brien, E. R. Williams, *J. Am. Chem. Soc.* **2012**, *134*, 10228–10236; f) J. S. Prell, J. T. O'Brien, E. R. Williams, *J. Am. Soc. Mass Spectrom.* **2010**, *21*, 800–809; g) T. Iino, K. Ohashi, Y. Mune, Y. Inokuchi, K. Judai, N. Nishi, H. Sekiya, *Chem. Phys. Lett.* **2006**, *427*, 24–28; h) T. Iino, K. Ohashi, K. Inoue, K. Judai, N. Nishi, H. Sekiya, *Eur. Phys. J. D* **2007**, *43*, 37–40; i) H. Ke, C. van der Linde, J. M. Lisy, *J. Phys. Chem. A* **2014**, *118*, 1363–1373; j) H. Ke, C. van der Linde, J. M. Lisy, *J. Phys. Chem. A* **2015**, *119*, 2037–2051; k) B. Bandyopadhyay, K. N. Reishus, M. A. Duncan, *J. Phys. Chem. A* **2013**, *117*, 7794–7803;

- [1] Y. Li, G. Wang, C. Wang, M. Zhou, *J. Phys. Chem. A* **2012**, *116*, 10793–10801.
- [17] B. J. Thomas, B. A. Harruff-Miller, C. E. Bunker, W. K. Lewis, *J. Chem. Phys.* **2015**, *142*, 174310.
- [18] a) E. Garand, T. Wende, D. J. Goebbert, R. Bergmann, G. Meijer, D. M. Neumark, K. R. Asmis, *J. Am. Chem. Soc.* **2010**, *132*, 849–856; b) A. Herburger, M. Ončák, C.-K. Siu, E. G. Demissie, J. Heller, W. K. Tang, M. K. Beyer, *Chem. Eur. J.* **2019**, *25*, 10165–10171; c) J. W. Shin, N. I. Hammer, M. A. Johnson, H. Schneider, A. Gloss, J. M. Weber, *J. Phys. Chem. A* **2005**, *109*, 3146–3152.
- [19] W. E. Thompson, M. E. Jacox, *J. Chem. Phys.* **1999**, *111*, 4487–4496.
- [20] P. Linstrom, *NIST Chemistry WebBook, NIST Standard Reference Database 69*; National Institute of Standards and Technology.
- [21] S. M. Craig, F. S. Menges, C. H. Duong, J. K. Denton, L. R. Madison, A. B. McCoy, M. A. Johnson, *Proc. Natl. Acad. Sci. USA* **2017**, *114*, E4706–E4713.
- [22] N. R. Walker, R. S. Walters, M.-K. Tsai, K. D. Jordan, M. A. Duncan, *J. Phys. Chem. A* **2005**, *109*, 7057–7067.
- [23] a) A. Chedin, *J. Mol. Spectrosc.* **1979**, *76*, 430–491; b) H. Günzler, H.-U. Gremlich, *IR-Spektroskopie: Eine Einführung*, Wiley-VCH, Weinheim, **2012**.
- [24] C. Berg, T. Schindler, G. Niedner-Schatteburg, V. E. Bondybey, *J. Chem. Phys.* **1995**, *102*, 4870–4884.
- [25] a) R. L. Wong, K. Paech, E. R. Williams, *Int. J. Mass Spectrom.* **2004**, *232*, 59–66; b) O. P. Balaj, C. B. Berg, S. J. Reitmeier, V. E. Bondybey, M. K. Beyer, *Int. J. Mass Spectrom.* **2009**, *279*, 5–9.
- [26] a) T. Schindler, C. Berg, G. Niedner-Schatteburg, V. E. Bondybey, *Chem. Phys. Lett.* **1996**, *250*, 301–308; b) R. C. Dunbar, *Mass Spectrom. Rev.* **2004**, *23*, 127–158.
- [27] N. C. Polfer, *Chem. Soc. Rev.* **2011**, *40*, 2211–2221.
- [28] E. Barwa, M. Ončák, T. F. Pascher, A. Herburger, C. van der Linde, M. K. Beyer, *Chem. Eur. J.* **2020**, *26*, 1074–1081.
- [29] C. M. Breneman, K. B. Wiberg, *J. Comput. Chem.* **1990**, *11*, 361–373.
- [30] M. J. Frisch, G. W. Trucks, H. B. Schlegel, G. E. Scuseria, M. A. Robb, J. R. Cheeseman, G. Scalmani, V. Barone, G. A. Petersson, H. Nakatsuji, et al., Gaussian 16, Revision A.03; Gaussian Inc, Wallingford CT, **2016**.

Manuscript received: January 24, 2020

Accepted manuscript online: February 26, 2020

Version of record online: March 12, 2020